Calculations for Gun Spectrometer

C. Limborg

October 15, 2003

Abstract

We discuss the transport through a system constituted of drift + bending magnet + drift. Parameters for obaining a point-to-point imaging in both the vertical and horizontal plane are derived. Numerical solutions are given.

0.1 Description

The gun spectrometer will be part of a relay imaging system designed to characterize the beam exiting the gun. A YAG1 screen has been positioned at 0.4 m from the cathode. The gun solenoid will be used as an optical element to image the cathode plane on this YAG1 screen indicating what is the uniformity of emission from the cathode. The system solenoid +YAG1 will also be used to characterize the intrinsic emittance ("thermal emittance") by performing solenoid scans. The spectrometer is being designed such that the beam at the location of YAG1 will itself will be imaged on to a YAG2 screen located after the spectrometer. Transverse properties along the bunch can then be measured such as the slice thermal emittance.

The spectrometer will primarily be used to measure longitudinal beam properties such as absolute energy, slice energy spread for low charge, correlated energy spread and current uniformity. These measurements will be described in details in another note.

In this note, we describe calculations for obtaining the point-to-point imaging and to get a high resolution power.

The resolution power has been defined in [Carey's "Optics of Charged Particles] P88].

1 Point to point imaging with sector magnet

1.1 Matrix analysis

We consider the bending magnet (wedge magnet) matrix M

$$M = \begin{bmatrix} \cos\left(\sqrt{1-n}\frac{L}{\rho}\right) & \frac{\rho}{\sqrt{1-n}}\sin\left(\sqrt{1-n}\frac{L}{\rho}\right) & \frac{\rho}{1-n}\left(1-\cos\left(\sqrt{1-n}\frac{L}{\rho}\right)\right) \\ -\frac{\sqrt{1-n}}{\rho}\sin\left(\sqrt{1-n}\frac{L}{\rho}\right) & \cos\left(\sqrt{1-n}\frac{L}{\rho}\right) & \frac{1}{\sqrt{1-n}}\sin\left(\sqrt{1-n}\frac{L}{\rho}\right) \\ 0 & 0 & 1 \end{bmatrix}$$

with n = 0 and α=$\frac{L}{\rho}$,

$$M = \begin{bmatrix} \cos(\alpha) & \rho\sin(\alpha) & \rho(1-\cos(\alpha)) \\ -\frac{1}{\rho}\sin(\alpha) & \cos(\alpha) & \sin(\alpha) \\ 0 & 0 & 1 \end{bmatrix}$$

For a drift of length L, the transport matrix is :

$$Drift(\ L) = \begin{bmatrix} 1 & L & 0 \\ 0 & 1 & 0 \\ 0 & 0 & 1 \end{bmatrix}$$

The transport to the screen is represented by R = Drift(L2) x M x Drift(L1), with L1 the distance from source to entrance bending magnet and L2 the distance from exit magnet to exit. For a point X_o =$(x_o, x_o\prime, \delta)$,the image X = RX_o is X$(x, x\prime, \delta)$.

$$\begin{aligned} x &= R_{11}x_o + R_{12}x'_o + R_{13}\delta \\ R_{11} &= \left[\cos(\alpha) - \frac{L_2\sin(\alpha)}{\rho}\right] \\ R_{12} &= \left[\cos(\alpha) - \frac{L_2\sin(\alpha)}{\rho}\right] L_1 + \rho\sin\alpha + L_2\cos\alpha \\ R_{13} &= \rho(1-\cos\alpha) + L_2\sin\alpha \end{aligned}$$

The resolving power $\mathcal{R}$ is defined by

$$\mathcal{R} = \frac{R_{13}}{2x_o R_{11}}$$

where x_o is the half-beam size

For a point-to-point imaging, the image position y does not depend on x'. Then $R_{12} = 0$, from which we derive

$$L_2 = -\frac{\rho\sin\alpha + L_1\cos\alpha}{\left[\cos(\alpha) - \frac{L_1\sin(\alpha)}{\rho}\right]}$$

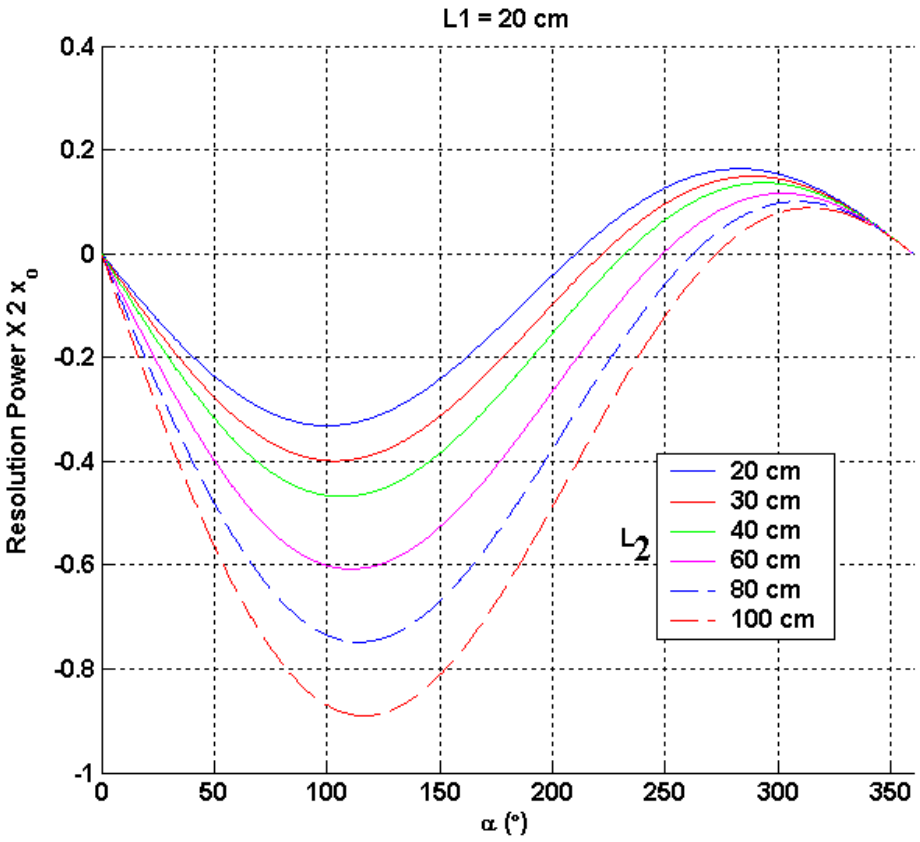

Figure 1:

then

$$R = \frac{\rho\left(1-\cos\alpha\right)+L_2\sin\alpha}{2x_o\left[\cos\left(\alpha\right)-\frac{L_2\sin(\alpha)}{\rho}\right]}$$

$$\begin{aligned} < \quad x^2 > &= R_{11}^2 < x_o^2 > + R_{13}^2 < \delta^2 > \\ \sigma_x \quad &= \quad R_{11}\sqrt{\sigma_{xo}^2 + \frac{R_{13}^2}{R_{11}^2}\sigma_\delta^2} \end{aligned}$$

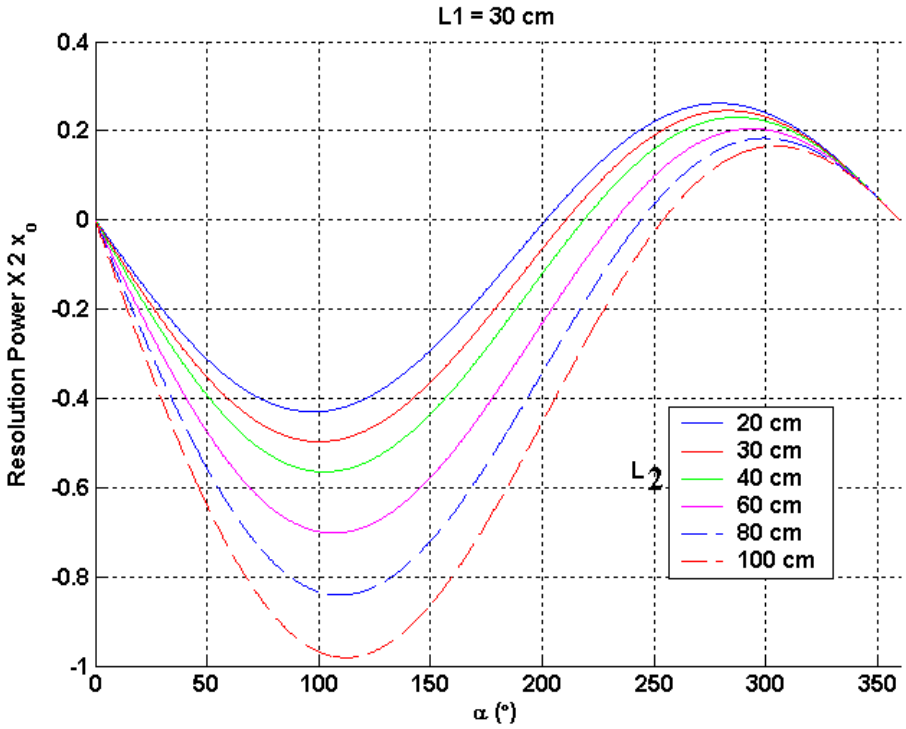
L1 = 30 cm
Resolution Power X 2 x0
α (°)
L2
20 cm
30 cm
40 cm
60 cm
80 cm
100 cm
0.4
0.2
0
-0.2
-0.4
-0.6
-0.8
-1
0
50
100
150
200
250
300
350

Figure 2:

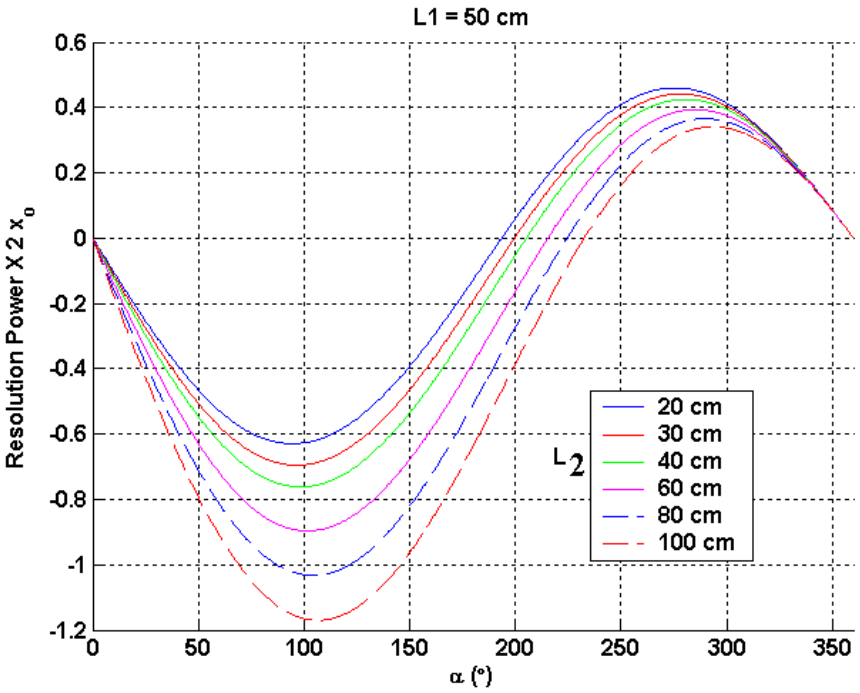
L1 = 50 cm
Resolution Power X 2 x0
0.6
0.4
0.2
0
-0.2
-0.4
-0.6
-0.8
-1
-1.2
0
50
100
150
200
250
300
350
α (°)
L2
20 cm
30 cm
40 cm
60 cm
80 cm
100 cm

Figure 3:

Assuming the half beam size x_o is 2 σ_{xo} ,

$$\sigma_x = R_{11}\sqrt{\sigma_{xo}^2\left(1+\left(4\mathcal{R}\right)^2\sigma_\delta^2\right)}$$

1.2 Numerics for minimum resolution

To resolve 10keV of a 5 MeV beam ($\sigma_\delta = 2.10^{-3}$), we need

$$\begin{aligned} 4\mathcal{R}\sigma_\delta &> 1 \\ \mathcal{R} &> 125 \end{aligned}$$

Assuming, $\sigma_{xo} < 2$ mm, $x_o < 4$ mm,

$$\mathcal{R} > 125.2.4.10^{-3} = 1$$

At 40 cm from the cathode (position of screen YAG1), and according to PARMELA simulations, σ_{xo} is in fact close to 1.78 mm.

The requirement for R_{13}/R_{11} should be larger than 0.89.

In figure1 and figure2, we see that R_{13}/R_{11} is always smaller than 0.89. In figure 3, we see that there exist solutions providing R_{13}/R_{11} larger than 0.89.

In Paragraph 2, we will solve directly for a point-to-point imaging in both horizontal and vertical planes. We will then find a solution for L1 = 0.4m.

1.3 Numerics for beam size extension

Let's assume that parameters are chosen for a R_{13}/R_{11}=0.89.

For a 250 keV rms relative beam energy spread ($\sigma_\delta = 5.10^{-2}$), the beam extension is :

$R_{11}(\sigma_{xo}^2 + \frac{R_{13}^2}{R_{11}^2}\sigma_\delta^2)^{1/2} = R_{11}\left((1.79.10^{-3})^2 + (0.89*5.10^{-2})^2\right)^{1/2} = 44.6$ mm R_{11}

The image will be too large to be captured on the screen.

The good energy resolution will be obtained at the expense of of large beam size. In revision 1, we will discuss a solution which includes an additional quadrupole. With that quadrupole, the dispersion can be reduced and the image will fit the screen.

2 Point-to-point imaging including pole face rotation to sector magnet

2.1 Matrix analysis

For treating the case of the pole face rotation we use 6x6 matrices.

with n = 0 and α=$\frac{L}{\rho}$,

$$M = \begin{bmatrix} \cos(\alpha) & \rho\sin(\alpha) & 0 & 0 & 0 & \rho(1-\cos(\alpha)) \\ -\frac{1}{\rho}\sin(\alpha) & \cos(\alpha) & 0 & 0 & 0 & \sin(\alpha) \\ 0 & 0 & 1 & \rho\alpha & 0 & 1 \\ 0 & 0 & 0 & 1 & 0 & 0 \\ -\sin(\alpha) & \rho(\cos(\alpha)-1) & 0 & 0 & 1 & -\rho(\alpha+\sin(\alpha)) \\ 0 & 0 & 0 & 0 & 0 & 1 \end{bmatrix}$$

The pole face rotation matrix is

$$P = \begin{bmatrix} 1 & 0 & 0 & 0 & 0 & 0 \\ \frac{\tan(\beta)}{\rho} & 1 & 0 & 0 & 0 & 0 \\ 0 & 0 & 1 & 0 & 0 & 0 \\ 0 & 0 & -\frac{\tan(\beta-\psi}{\rho}) & 1 & 0 & 0 \\ 0 & 0 & 0 & 0 & 1 & 0 \\ 0 & 0 & 0 & 0 & 0 & 1 \end{bmatrix}$$

We assume the same angle for the entrance and exit pole faces. The transport natrix is then R = Drift(L2) x P x M x P x Drift(L1).

The coefficients of interest are

$$\begin{aligned} R_{11} &= \cos\alpha - \frac{L_2\sin\alpha}{\rho} + \frac{\tan\beta}{\rho}(\rho\sin\alpha + 2L_2\cos\alpha) + \frac{\tan^2\beta}{\rho^2}\rho L_2\sin\alpha \\ R_{12} &= (L_1+L_2)\cos\alpha + \left(\rho - \frac{L_1L_2}{\rho}\right)\sin\alpha + \frac{\tan\beta}{\rho}\left[\rho\sin\alpha\,(L_1+L_2) + 2L_1L_2\cos\alpha\right] \\ &\quad +\rho\sin\alpha L_1L_2\frac{\tan^2\beta}{\rho^2} \\ R_{16} &= \rho(1-\cos\alpha) + L_2\sin\alpha + \frac{\tan\beta}{\rho}L_2\rho(1-\cos\alpha) \\ R_{33} &= 1 + \alpha\rho L_2\frac{\tan^2(\beta-\psi)}{\rho^2} - \frac{\tan(\beta-\psi)}{\rho}(2L_2+\rho\alpha) \\ R_{34} &= L_1 + L_2 + \rho\alpha(1 + L_1L_2\frac{\tan^2(\beta-\psi)}{\rho^2}) - \frac{\tan(\beta-\psi)}{\rho}((L_1+L_2)\rho\alpha + 2L_1L_2) \end{aligned}$$

$$
\begin{aligned}
R_{11} &= \cos\alpha - \frac{L_2\sin\alpha}{\rho} + \tan\beta(\sin\alpha + \frac{2L_2\cos\alpha}{\rho}) + \tan^2\beta\frac{L_2\sin\alpha}{\rho} \\
R_{12} &= \left(\cos\alpha - \frac{L_2\sin\alpha}{\rho}\right) L_1 + \rho\sin\alpha + L_2\cos\alpha + \tan\beta\left[(L_1+L_2)\sin\alpha + \frac{2L_1L_2\cos\alpha}{\rho}\right] \\
&\quad + \sin\alpha L_1 L_2\frac{\tan^2\beta}{\rho} \\
R_{16} &= \rho(1-\cos\alpha) + L_2\sin\alpha + \tan\beta(1-\cos\alpha)L_2 = (1-\cos\alpha)(\rho + L_2\tan\beta) + L_2\sin\alpha \\
R_{33} &= 1 + \alpha L_2\frac{\tan^2(\beta-\psi)}{\rho} - \frac{\tan(\beta-\psi)}{\rho}(2L_2 + \rho\alpha) \\
R_{34} &= L_1 + L_2 + \rho\alpha(1 + L_1L_2\frac{\tan^2(\beta-\psi)}{\rho^2}) - \frac{\tan(\beta-\psi)}{\rho}((L_1+L_2)\rho\alpha + 2L_1L_2)
\end{aligned}
$$

One can also write

$$
\begin{aligned}
R_{12} &= \left(\cos\alpha - \frac{2L_2\sin\alpha}{\rho}\right) L_1 + \rho\sin\alpha + L_2\cos\alpha + \tan\beta\left[\sin\alpha\,(L_1+L_2) + \frac{2L_1L_2\cos\alpha}{\rho}\right] \\
&\quad + \frac{\sin\alpha L_1L_2}{\rho}\tan^2\beta \\
R_{12} &= L_2\left[\cos\alpha - 2\frac{L_1}{\rho}\sin\alpha + \tan\beta\left[\sin\alpha + 2\frac{L_1\cos\alpha}{\rho}\right] + \tan^2\beta\frac{\sin\alpha L_1}{\rho}\right] \\
&\quad + \rho\sin\alpha + L_1\left[\cos\alpha + \tan\beta\sin\alpha\right]
\end{aligned}
$$

$$
R_{34} = L_2\left[1 + \alpha\frac{L_1}{\rho}\tan^2(\beta-\psi) - \tan(\beta-\psi)\left(\alpha + 2\frac{L_1}{\rho}\right)\right] + \rho\alpha + L_1(1 - \alpha\tan(\beta-\psi))
$$

For a point-to-point imaging system in both planes, both $R_{12} = 0$ and $R_{34} = 0$.

From R_{12}=0,

$$
L_2 = -\frac{\rho\sin\alpha + L_1\left[\cos\alpha + \tan\beta\sin\alpha\right]}{\left[\cos\alpha - \frac{L_1}{\rho}\sin\alpha + \tan\beta\left[\sin\alpha + 2\frac{L_1}{\rho}\cos\alpha\right] + \tan^2\beta\sin\alpha\frac{L_1}{\rho}\right]}
$$

From R_{34}=0,

$$
L_2 = -\frac{\rho\alpha + L_1(1 - \alpha\tan(\beta-\psi))}{\left[1 + \alpha\frac{L_1}{\rho}\tan^2(\beta-\psi) - \tan(\beta-\psi)\left(\alpha + 2\frac{L_1}{\rho}\right)\right]}
$$

We first assume that $\psi = 0$.

If we assume $\beta = 25°$

Again the resolving power is defined by

$$\mathcal{R} = \frac{R_{16}}{2x_o R_{11}}$$

with $2x_o$ the beam size at the source
Then,

$$\mathcal{R} = \frac{(1-\cos\alpha)(\rho + L_2\tan\beta) + L_2\sin\alpha}{2x_o\left[\cos\alpha - \frac{L_2\sin\alpha}{\rho} + \tan\beta(\sin\alpha + \frac{2L_2\cos\alpha}{\rho}) + \tan^2\beta\frac{L_2\sin\alpha}{\rho}\right]}$$

The resolving power can be maximized by introducing a slit which reduces the x_o value. In our design, we have not included the possibility of inserting a slit. If it's proven to be necessary at a later date, this option will be considered.

2.2 Numerical solution

A Matlab solver was written to find numerical solutions giving $R_{12} = R_{34} = 0$. The results are presented in figure 4. Obviously, those results don't include space charge effects and include only linear optics calculation. Numerical values are given in Table 1.

The constraints are for our best solution are:
- good resolving power so R_{16}/R_{11}large
- not too large image R_{16} not too large

- L2 should not be too small to accomodate the T tank for the measurement screen.

The optimal cases are given in Table1.1. Those values were checked using MAD. The second order coefficients were then extracted.

β	L_1	L	L_2	α	R_{16}(m)	T_{166}	T_{116}	T_{126}	T_{336}	T_{346}
25	0.3	0.2	0.2723	86	0.5	-0.57	1.75	0.55	1.037	0.77
30	0.3	0.25	0.212	98.39	0.51	-0.55	1.79	0.603	0.32	0.603
30	0.3	0.3	0.3063	98.21	0.705	-0.793	2.02	0.67	0.33	0.83
30	0.4	0.3	0.227	98.683	0.576	-0.601	1.67	0.755	0.312	0.670

Table 1.1- Numerical solution for point-to-point focusing in both horizontal and vertical planes. The second order coefficients were computed using MAD.

2.3 Effect of fringe field

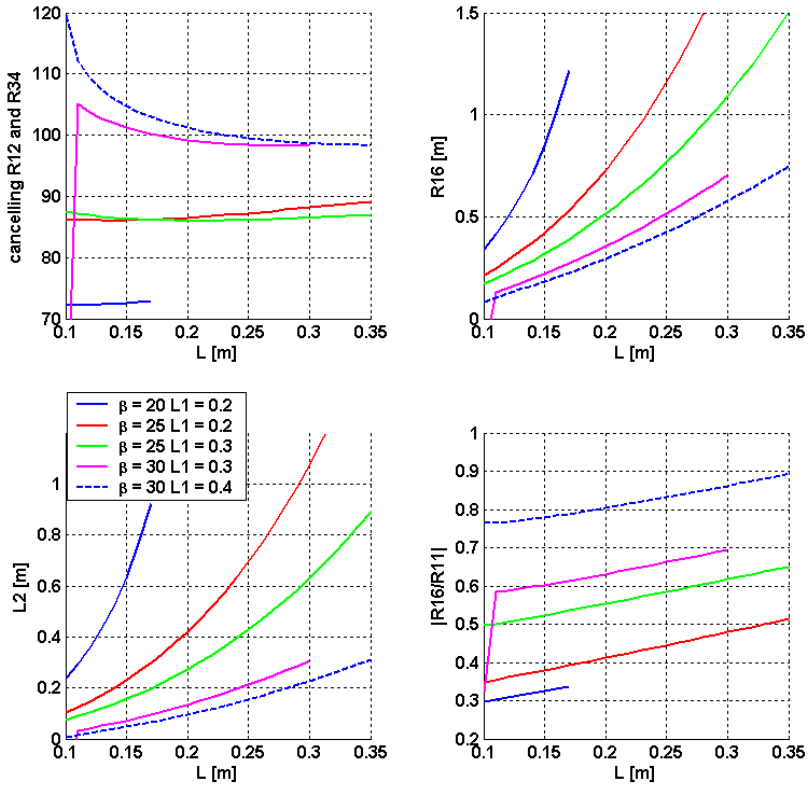

Figure 4: Numerical Solution from Matlab Solver; The computation only includes linear optics and no space charge

2.3.1 Analytic formula for fringe field ψ

From K.Brown [TRANSPORT manual], the fringe field is given by

$$\begin{aligned} \psi &= K_1 \frac{g}{\rho_o} \frac{1+\sin^2\beta}{\beta} \left[1 - K_1 K_2 \frac{g}{\rho_o} \tan\beta\right] \\ g &: \text{total gap of magnet} \\ \beta &: \text{angle of rotation of pole face} \\ \rho_o &: \text{bending radius} \\ & \quad K_1 \text{ and } K_2 \text{ tabulated for magnet family} \end{aligned}$$

We use $g = 1$ inch for the total gap and K1 = 0.45, K2 = 2.8 (for a sqaure edged magnet).

2.3.2 Numerical solution

Since we solve in α , we don't know what is ρ. Solving the problem in a self-consistent way is difficult and not very useful here. ρ was deduced by solving with $\psi = 0$ and then injected in the solver. It was then checked that the ψ value did not vary much. This is shown in figure 5.

The bending angle and resolving power do not change when including the fringe field. The dispersion increases. The distance from bending magnet exit to screen is slightly increased.

The numerical solution obtained with our Matlab solver is given in figure 6. The optimal cases were then computed with MAD. Those results are summarized in the table below, which also show the second order coefficients:

β	L_1	L	L_2	α	R_{16}(m)	T_{166}	T_{116}	T_{126}	R_{11}	R_{33}	T_{336}	T_{346}
25	0.3	0.2	0.3879	82.63	0.6515	-0.75	2.00	0.6	-1.21	-1.4	1.39	1.06
30	0.3	0.25	0.284	95.11	0.623	-0.723	2.01	0.64	-0.97	-1.12	0.42	0.8
30	0.3	0.3	0.399	95.47	0.846	-1.01	2.273	0.723	-1.245	-1.32	0.43	1.08
30	0.4	0.3	0.298	95.48	0.684	-0.766	1.853	0.804	-0.81	-1.00	0.39	0.878

Table 2.1- Numerical solution for point-to-point imaging including fringe field effects.

2.3.3 Quantification of Second Order Effects

The second order coefficients are negligeable. The interested reader can check it by himself.

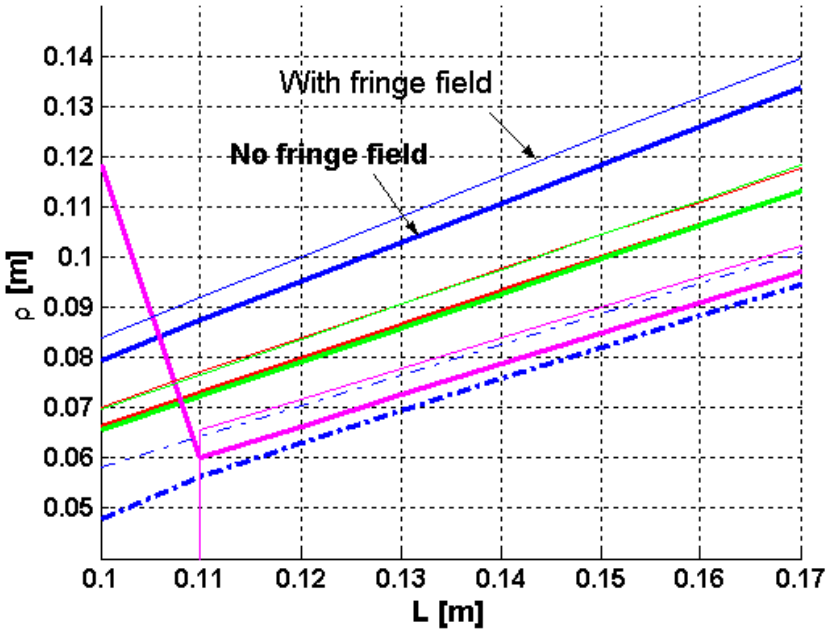

Figure 5: Self-Consistent solution for numerical model including fringe field

Case of $\mathbf{T}_{166}$ T_{166} will possibly contribute to the beam size.

For a 1nC bunch, with the typical LCLS parameters, the normalized rms energy spread is of 0.67% at the object and 1.32% at the image. At the object $\sigma_{xo} = 1.78$ mm.

The square of the rms beam size is given by: $R_{11}^2\sigma_{xo}^2 + R_{16}^2\sigma_\delta^2 + T_{166}^2 < \delta^4 >$
$< \delta^2 >= 4.49.10^{-5}, \sigma_\delta = 0.67\%, \quad < \delta^4 >= 9.19.10^{-9}$ at object point
$< \delta^2 >= 1.75.10^{-4}$, σ_δ =1.32%, $< \delta^4 >= 1.24.10^{-7}$ at image point
The expected beam size is for case 1
$1.21^2 1.78^2 + 0.65^2\ 44.9 + 0.75^2\ 9.2.10^{-3} = 4.63 + 18.9 + 0.0052$

Case of $\mathbf{T}_{366}$ The square of the vertical beam size is $\sigma_y^2 = R_{33}^2\sigma_{yo}^2 + T_{366}^2 < \delta^4 >$
Using the values from case 1 of Table 2, $\sigma_y^2 = 1.4^2 1.22^2 + 1.39^2\ 0.124 = 6.4$. The vertical beam size is 1.53 mm and T_{366} is negligeable.

3 Simulations with PARMELA

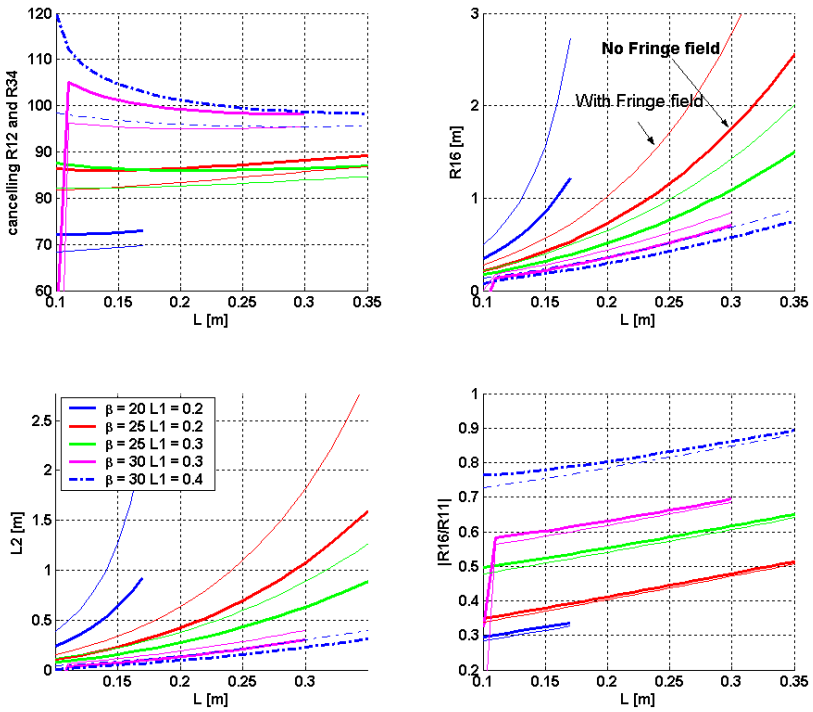

Figure 6: Numerical Solution for point-to-point imaging; the model includes fringe field effects

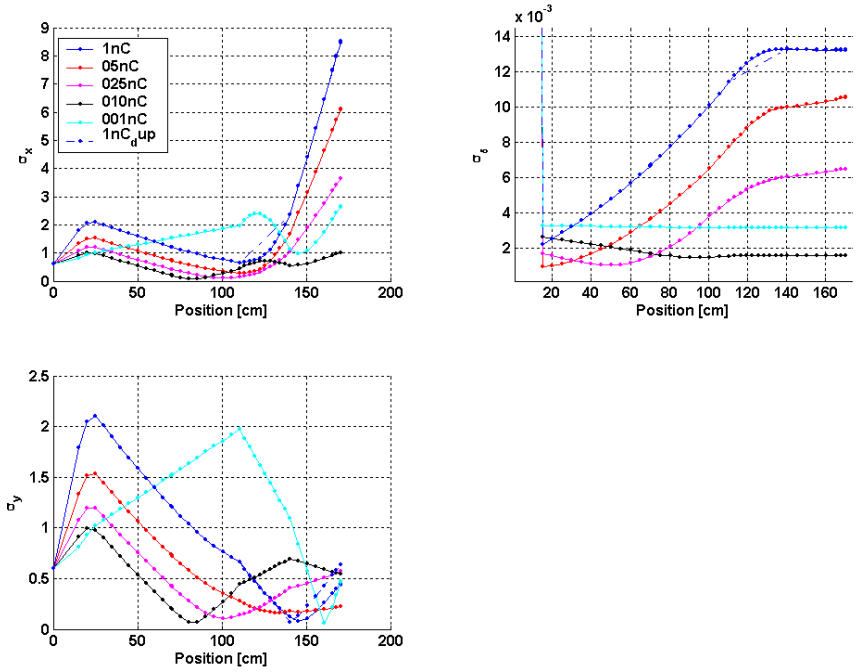

Figure 7: PARMELA run; rms beam sizes are given in mm

The standard LCLS parameters from the 2002 tuning were used.

Vrf	Φ	r	Q	σ_{rise}
120MV/m	27	1.2 mm	1nC	0.5ps

The PARMELA runs shown in figure 7 were performed for case 4 of table1.1 with 98.6 degrees bend and 30 degrees for pole face rotation. The beam sizes at the spectrometer screen are given in mm. For low charges, the image will be contained on the screen. For high charges, the horizontal rms beam size will be as large as 9mm and the image will exceed the screen dimension. (The possibility of reducing the dispersion and so the horizontal beam size will be discussed in the next note). In those simulations YAG1 had been located at 70.1cm from the cathode. YAG1 had been later moved to 40 cm from the cathode.